Current Trends in Technology and Science
ISSN: 2279- 0535. Volume: 3, Issue: 5 (Aug-Sept. 2014)

Effect of Doping Level of a Silicon Solar Cell Under Back Side Illumination

[1]Khady FAYE, [1]Idrissa GAYE, [1]Sega GUEYE, [2]Seni TAMBA, [1]Gregoire SISSOKO (gsissoko@yahoo.com)
[1]Laboratory of Semiconductors and Solar Energy, Physics Department, Faculty of Science and Technology
University Cheikh Anta Diop – Dakar – SENEGAL.
[2] Electromechanical Engineering Department, Polytechnic School of Thies – SENEGAL

Abstract - A theoretical study of a silicon solar cell under polychromatic illumination and under base doping rate is presented for the back surface illumination mode. An analysis of the effects of base doping rate on the minority carriers density, and we show how the photocurrent, the photovoltage, the capacity, the short-circuit photocurrent density, and the open-circuit photovoltage depend on base doping. Either the I-V characteristic, series and shunt resistances are determined and studied versus doping rate.

Keywords - Doping rate; silicon solar cell, Shunt and Series resistances.

I. INTRODUCTION

The doping of semiconductors is important for the manufacturing of electronic components. The interesting electronic properties are thus connected to the possibility of "doping" of material by the introduction of adequate impurities allowing introducing free carriers. Seen importance of doping, we suggested to study in static regime, the base of a silicon solar cell under constant spectral multi-illumination and under the influence of the doping rate. The study is limited to illumination by back side surface where the phenomena of recombination are very important, We look first at the influence of doping rate and at the minority carriers density, Then we are interested at its effects on the photocurrent density, the photovoltage, the capacity, the short-circuit photocurrent and the open circuit photovoltage. We also look at the effects of doping rate on series and shunt resistances, from study of the I-V characteristic **[1]-[2]**.

II. THEORETICAL STUDY

A n^+-p-p^+ silicon solar cell type **[1]-[3]** is schematized on figure 1:

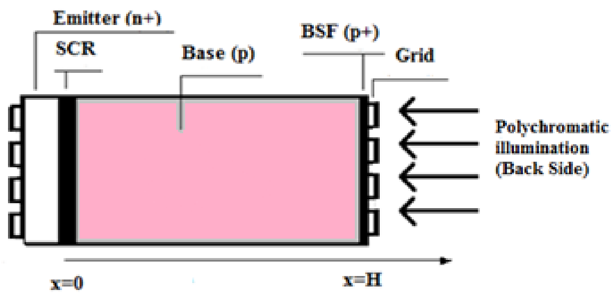

Figure 1: n^+pp^+ Silicon Solar cell

When the solar cell is illuminated, different process take place in the base: We can mention generation, recombination and diffusion of excess minority carriers. The continuity equation for all these phenomena in static regime is given by the expression below:

$$\frac{\partial^2 \delta(x)}{\partial x^2} - \frac{\delta(x)}{L^{*2}} = -\frac{G(x)}{D^*} \qquad (1)$$

G(x) is the carrier generation rate.

Under back side illuminated, the expression of generation rate is given by the relation (2): The silicon solar cell is used in static regime

$$G(x) = n \cdot \sum_{i=1}^{3} a_i \cdot \exp(-b_i (H - x)) \qquad (2)$$

a_i and b_i are coefficients deduced from solar radiation under AM 1,5 spectrum **[4]**;

We set n = 1 (Number of sun).

D*(Nb) indicates diffusion coefficient (Which translates the more or less good capacity of the material to let broadcast the carriers) of electrons generated in the base. The diffusion coefficient depends on base doping rate by the following relation **[5]-[6]-[7]**:

$$D^*(Nb) = \frac{1350 \cdot V_T}{\sqrt{1 + 81 \cdot \dfrac{N_b}{N_b + 3{,}2 \cdot 10^{18}}}} \qquad (3)$$

Where V_T is the thermal voltage.

The diffusion length L* of the excess minority carriers depends on doping rate by the following expression:

$$L^*(Nb) = \sqrt{D^*(Nb) \cdot \tau(Nb)} \qquad (4)$$

τ(Nb) is the minority carriers lifetime.

It is given by equation (5) **[8]**:

$$\tau(Nb) = \frac{12}{1+\dfrac{Nb}{5\times 10^{16}}} \qquad (5)$$

The general solution of continuity equation is given by the expression (6):

$$\delta(x) = A\cdot\cosh(\frac{x}{L*}) + B\cdot\sinh(\frac{x}{L*}) - \sum_{i=1}^{3}\frac{n\cdot a_i\cdot L*^2}{D*\cdot(b_i\cdot L*^2-1)}\cdot\exp(-b_i\cdot(H - \quad (6)$$

With coefficients A and B the final solution of the continuity equation is well known **[9]-[10]**.

These coefficients can be determined through the following boundary conditions:

At the junction (x = 0)

$$D*\cdot\frac{\partial\delta(x)}{\partial x}\Big|_{x=0} = Sf\cdot\delta(x)\Big|_{x=0} \qquad (7)$$

At the back surface (x = H):

$$D*\cdot\frac{\partial\delta(x)}{\partial x}\Big|_{x=H} = -Sb\cdot\delta(x)\Big|_{x=H} \qquad (8)$$

Where H is the total thickness of the solar cell,

Sf and Sb are respectively junction recombination velocity and back side recombination velocity;

Back side recombination velocity depends on doping rate. To determine Sb we use the following relation [10]:

$$\frac{\partial Jph}{\partial Sf} = 0 \qquad (9)$$

Where Jph is the photocurrent density;

After calculation we find the following expression:

$$Sb(Nb) = \frac{D^*(Nb)}{L^*(Nb)}\cdot\sum_{i=1}^{3}\left(\frac{b_i.L^*(Nb).e^{-b_i.H} + \sinh(\frac{H}{L^*(Nb)}) - b_i.L^*(Nb).\cosh(\frac{H}{L^*(Nb}}{e^{-b_i.H} - \cosh(\frac{H}{L^*(Nb}) + b_i.L^*(Nb).\sinh(\frac{H}{L^*(Nb)})}\right. \qquad (10)$$

Figure 2 shows the module of back side recombination velocity versus doping rate:

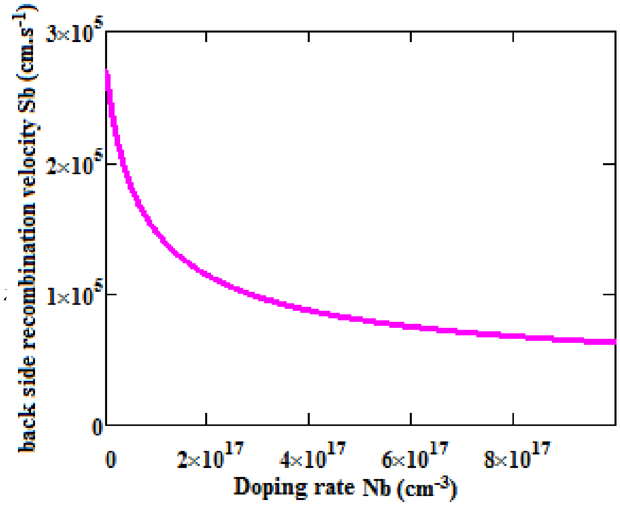

Figure 2: back side recombination velocity versus doping rate

The back side recombination velocity decrease with the doping rate

III. Results and Discussions

III-1 Excess minority carriers density

On figure 3, we give profile of minority carriers density versus depth for various base doping rates:**[11]**

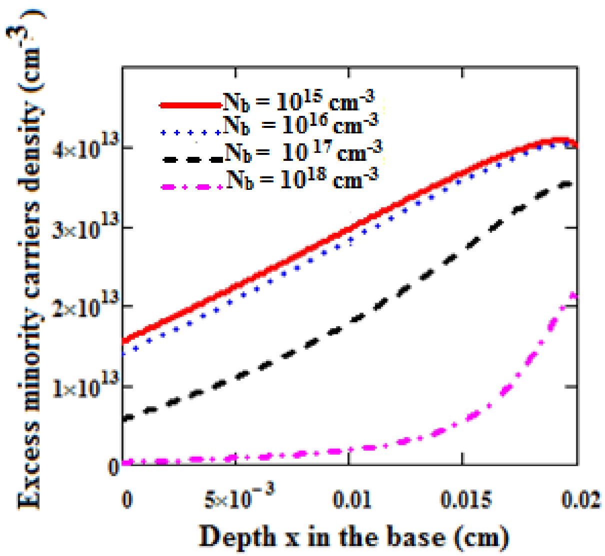

Figure 3: Minority carriers Density in the base versus depth for various base doping rates: Sf = 3.10^3cm.S^{-1}

On figures 2 and 3, we observe that the minority carriers' density decreases with base doping rate. It's especially marked for the strong doping of the base. Indeed, if the base doping increases, it means that the impurities within the material increase: This entails an

Current Trends in Technology and Science
ISSN: 2279- 0535. Volume: 3, Issue: 5 (Aug-Sept. 2014)

increase of recombinations in volume and consequently a decrease of the density of these carriers.

We notice also an increase of the density with the depth x in the base.

III-2 Photocurrent density

The photocurrent density of the solar cell is obtained by the gradient of minority carriers at the junction and is given by the following expression:

$$J_{ph} = q \cdot D^* \cdot \frac{\partial \delta(x)}{\partial x}\Big|_{x=0} \qquad (11)$$

Where q is the elementary charge.

Figure 4 illustrates variation of photocurrent density versus junction recombination velocity for different values of doping rate:

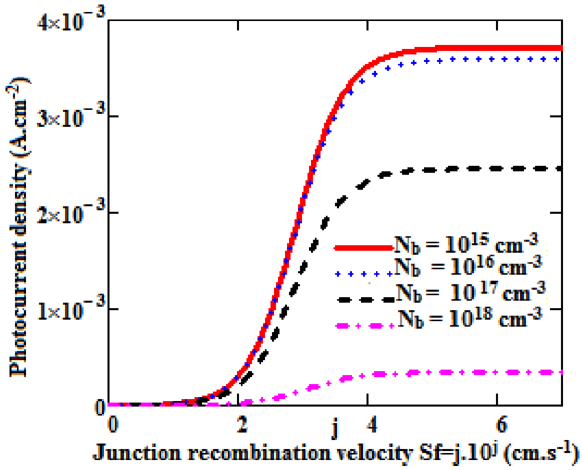

Figure 4: Photocurrent density versus junction recombination velocity for different doping rates

We observe that photocurrent density increases with junction recombination velocity with a maximum value near short circuit. The photocurrent density decreases very quickly with base doping rate: The back side of the solar cell is very sensitive to doping rate.

III-2-1 Short-circuit photocurrent

We present in *figure 5* the effect of doping rate on short-circuit photocurrent density:

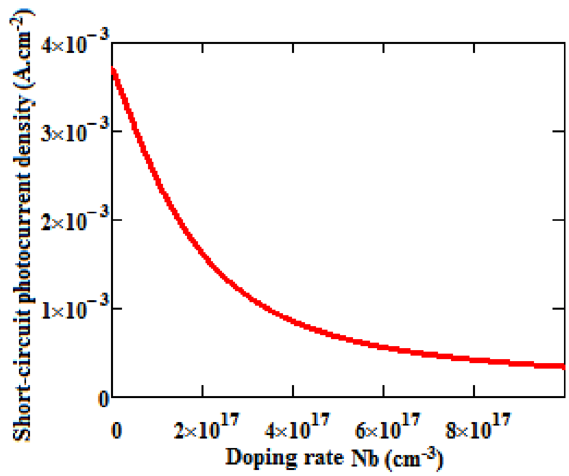

Figure 5: Short-circuit photocurrent density according to doping rate

We can observe that the short-circuit photocurrent decreases with doping rate of the base.

III-3 Photovoltage

From Boltzmann law, the photovoltage can be written as:

$$V_{ph} = V_T \cdot \ln\left(1 + \frac{N_b}{n_i^2} \cdot \delta(x)\big|_{x=0}\right) \qquad (12)$$

$$V_T = \frac{K_b \cdot T}{q} \qquad (13)$$

V_T is the thermal voltage; n_i is the intrinsic concentration of the minority carriers K_b is the Boltzman constant (1,38.10^{-23}m^2. Kg.S^{-2}.K^{-1});

T is the absolute temperature.

We present in figure 6 the profile of photovoltage versus junction recombination velocity for different doping level:

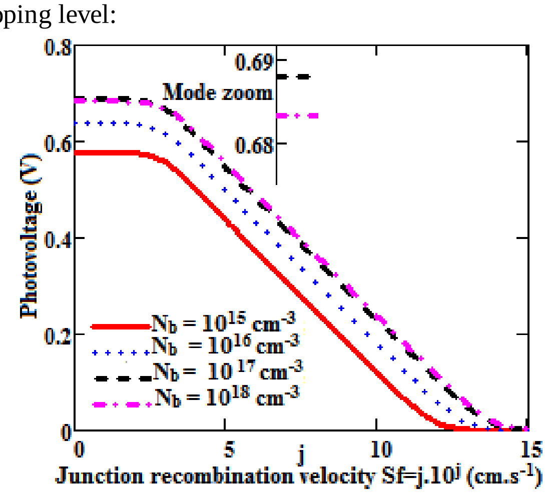

Figure 6: Photovoltage versus junction recombination velocity for different doping rate

Current Trends in Technology and Science
ISSN: 2279- 0535. Volume: 3, Issue: 5 (Aug-Sept. 2014)

We observe that photovoltage increases with doping rate. It is interpreted by decreasing of diffusion coefficient with base doping rate. Also the space charge zone width is inversely proportional to base doping rate. When the doping of the base increases, the width of space charge region decreases, fewer carriers are collected by the junction.

III-3-1 Open circuit photovoltage

On figure 7 is represented the profile of open circuit photovoltage according to the base doping level :

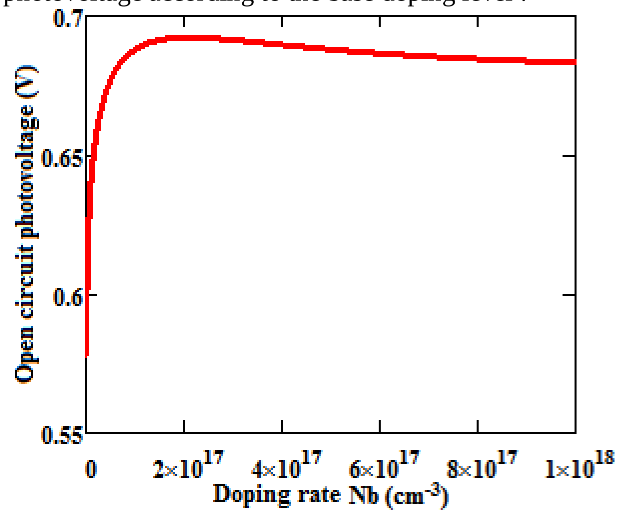

Figure 7: Open circuit photovoltage versus doping rate

The open circuit photovoltage increases with doping rate for values between 10^{15} and 10^{17} cm^{-3}, beyond 10^{17} cm^{-3} it decreases.

III-4 I-V Characteristic

Profile of I-V characteristic for various doping level is given on figure 8:

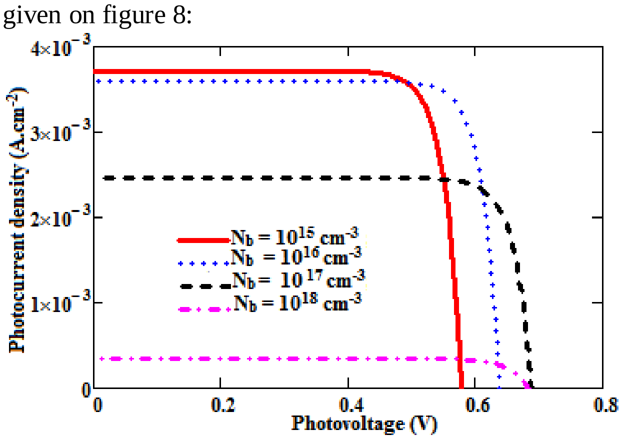

Figure 8: I-V Characteristic for various doping level

This figure shows that near short-circuit, the photovoltage is low, the current is there almost constant and corresponds at short-circuit current. When the photovoltage aims towards open circuit photovoltage, the photocurrent decreases to nullify.

III-5 Study of series and shunt resistances

For the I-V characteristic of the solar cell we are going to determine some electrical parameters of the solar cell such as series and the shunt resistances.

II-5-1 Series Resistance

The series resistance Rs is a fundamental parameter which depends on nature of substratum, on temperature, on used technology and plays a role determining on the quality of a solar cell. It characterizes the contacts resistance, the resistivity of the base material. For a front illumination, the series resistance is often very small. Contrariwise as we can notice it on figure 10, for the back surface illumination we obtain higher values of series resistance, since excess minority carriers generated at the back side must travel along the base depth before crossing the junction.

On the characteristic current-tension of solar cell we obtain two operating points, It is about open circuit situation where the photovoltage is maximal and short-circuit situation where the photocurrent is maximal.

In this study, for determining the series resistance Rs, we propose the equivalent electrical model of the solar cell in open circuit (low values of Sf) where the solar cell operates as photovoltage generator associated to series resistance and the external load (Rch) [12]-[13].

The equivalent electrical model of the solar cell near open circuit is represented below:

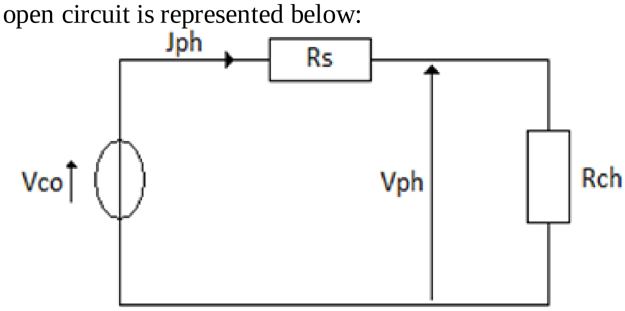

Figure 9: Equivalent electrical model of the solar cell near open circuit situation

By applying the law of meshs to the circuit of figure 9, we find the expression of series resistance:

$$R_S = \frac{V_{phco} - V_{ph}(Sf)}{J_{ph}(Sf)} \qquad (14)$$

R_S and Rch are respectively series and charge resistance.

Sf aims towards Sfco which is junction recombination velocity limiting the open circuit**[14]**. On figure 10, we give the profile of series resistance versus junction recombination velocity for various doping rate:

Current Trends in Technology and Science
ISSN: 2279- 0535. Volume: 3, Issue: 5 (Aug-Sept. 2014)

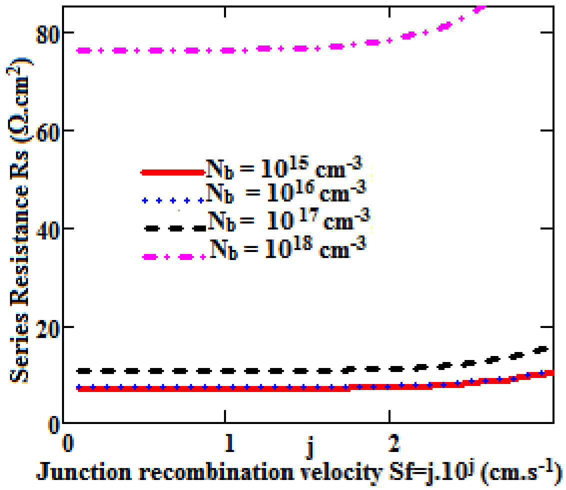

Figure 10: Series Resistance versus junction recombination velocity for various doping level

We note that at open circuit situation, the series resistance increases gradually with the junction recombination velocity. We also observe that the series resistance increases with doping rate of the base. We can thus conclude that the resistivity of the material increases with the doping.

III-5-2 Shunt resistance

The shunt resistance R_{Sh} characterizes current losses at the junction. It allows to appreciate the quality of the solar cell. To determine the shunt resistance, we propose the equivalent electrical model of the solar cell near short circuit (larges values of Sf (4.10^4cm.s^{-1}< Sf < 6.10^6 cm.s^{-1}). The illustrative model of this device is given to figure 11

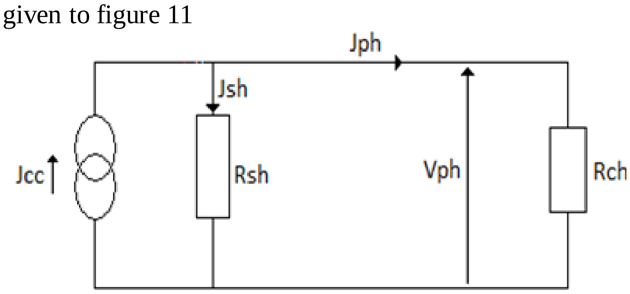

Figure 11: Equivalent electrical model of the solar cell near short-circuit

By applying the nodes law to the circuit 11, we find the expression of the shunt resistance datum in the relation 15:

$$R_{Sh} = \frac{V_{ph}(Sf)}{J_{phcc} - J_{ph}(Sf)} \qquad (15)$$

J_{phcc} is the short-circuit photocurrent; it's determined from the following relation:

$$J_{phcc} = \lim_{Sf \to \infty} J_{ph} \qquad (16)$$

R_{Sh} and R_{ch} are respectively shunt and charge resistance.

Sf aims towards Sfcc which is the recombination velocity at junction initiating the short-circuit **[14]**; the profile of the shunt resistance versus recombination velocity at junction for various values of doping rate is given at the figure 12:

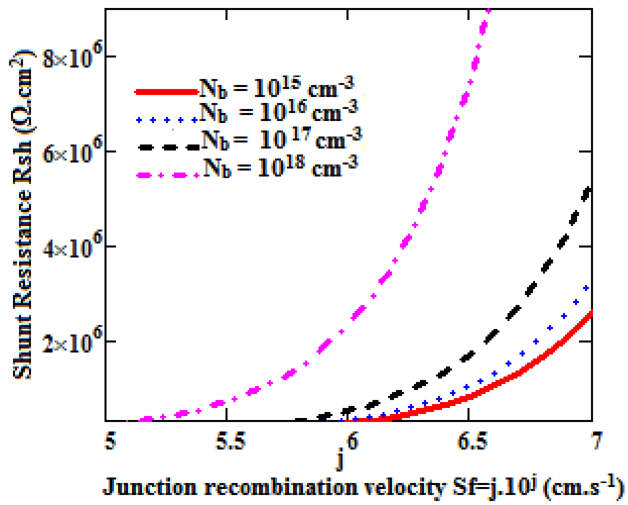

Figure 12: Shunt resistance versus junction recombination velocity at junction for various doping rate

We note an increase of the shunt resistance with the recombination velocity at junction. The shunt resistance also increases with the base doping rate.

III-6 The capacity

The capacity is obtained from the following expression:

$$C = \frac{\partial Q}{\partial V_{ph}} \qquad (17)$$

After calculation, we find the following expression:

$$C = C_0 + \frac{q \cdot \delta(0)}{V_T} \qquad (18)$$

With

$$C_0 = \frac{q \cdot \frac{ni^2}{Nb}}{V_T} \qquad (19)$$

C_0 is the intrinsic capacity without illumination and without base doping.

We give on figure 13 the profile of the capacity versus recombination velocity at junction for various doping rate of the base:

Current Trends in Technology and Science
ISSN: 2279- 0535. Volume: 3, Issue: 5 (Aug-Sept. 2014)

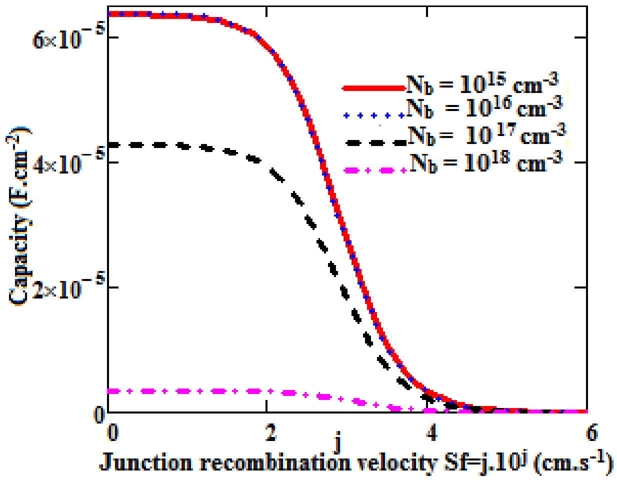

Figure 13: Capacity versus recombination velocity at junction for various doping rate

We observe on figure 13 that the capacity decreases with the junction recombination velocity (Sf). When Sf increases, the minority carriers cross the junction to participate at the photocurrent: what decreases the storage of these carriers near the junction. The recombinations of carriers increase with the doping of the base, what induce a decrease of the minority carriers stored thus a decrease of the capacity **[15]**. The profile of the logarithm of the capacity versus photovoltage for various doping rate is represented at figure 14:

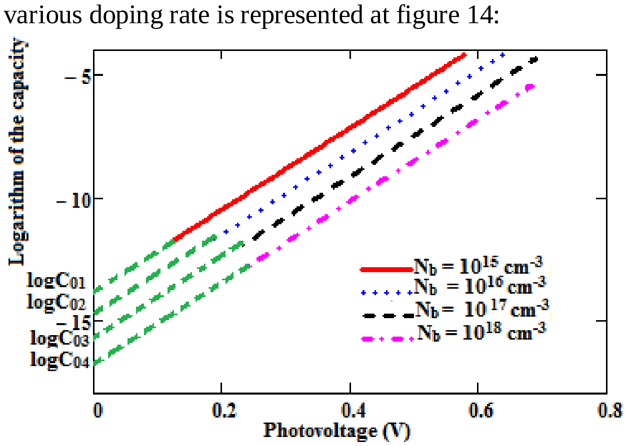

Figure 14: Logarithm of the capacity versus photovoltage for various doping rate of the base

These curves (Figure 14) present a linear evolution. The capacity increases with the photovoltage at the boundaries of the solar cell and decreases with doping rate of the base. For every rate of doping we have a particular value of the intrinsic capacity because it only depends on the level of doping and on the temperature.

Table 1: Intrinsic values of capacity for various doping level under back side illumination:

values of C_0 (F/cm^2)	
C_{01}	$1{,}19.10^{-6}$
C_{02}	$3{,}65.10^{-7}$
C_{03}	$1{,}35.10^{-7}$
C_{04}	$5{,}04.10^{-8}$

This table shows that the intrinsic capacity decreases with the doping of the base. Indeed, in relation 19, the intrinsic capacity is inversely proportional to doping.

IV. Conclusion

We presented in this work a theoretical study of a silicon solar cell in static regime, under constant spectral illumination and under the influence of base doping rate. The expression of the minority carriers density, for back side illumination was established. The profile of this density is represented versus the depth x in the base for various doping rate. This minority carriers density decreases with the base doping rate. The determination of the minority carriers density in the base of the solar cell, allowed us to have the expressions of the photocurrent and of the photovoltage. The I-V characteristic was represented, this allowed us to establish the expressions of series and shunt resistances following both modes of functioning of the solar cell (open circuit situation and short-circuit situation). Whose profiles were also studied according to the junction recombination velocity for various base doping rate. Either, the capacity study was made. From profiles of the logarithm of the capacity according to the photovoltage, we determined the intrinsic capacity without illumination, and we showed that the capacity decreases with the base doping rate.

References

[1] Daniel. L. Meier, Jeong-Mo Hwang, Robert B. Campbell. IEEE Transactions on Electron Devices, vol. ED-35, No.1, 1988, pp.70 – 78.

[2] P. H. Nguyen, C. Michel et J. Bottin Study of photovoltaic conversion: effects of parasitic resistances of solar cells. Revue Phys. Appl. 18 (1983) 775-779

[3] A. Hübner, A.G.Aberle, and R. Hezel 20% Efficient Bifacial Silicon Solar Cells, 14th European PVSEC, (Munich, 2001) pp 1796 – 1798.

[4] S. N. Mohammad, An alternative method for the performance analysis of silicon solar cells, J. Appl. Phys. Vol 61.N^0 2 767-772 1987

[5] J.J. Liou, W.W. Wong, Comparison and optimization of the performance of Si and GaAs solar cells, Solar Energy Materials and Solar Cells Volume 28, Issue 1, 1992, pp.9–28

[6] G. Sissoko, E. Nanema, Y. L. B. Bocande, A. L. Ndiaye, M. Adj Minority Carrier Diffusion Length Measurement In Silicon Solar Cell Under Constant White Biais Light. World Renewable Energy Congress (WREC), Vol. 3, pp 1598-1601, 1996, Elsevier Science Ltd.

[7] Amadou Diao, Ndeye Thiam, Martial Zoungrana, Gokhan Sahin, Mor Ndiaye, Grégoire Sissoko Diffusion coefficient in Silicon Solar Cell with applied magnetic field and under frequency: electric equivalent circuits. World Journal of Condensed Matter Physics, 2014, 4, 84-92.

[8] G. Sissoko, A. Fickou, M. Kane, P. Mialhe. Experimental determination of minority carrier lifetime and diffusion coefficient in solar cells. Workshop for planning of network projects in material sciences and solar energy, Nairobi, Kenya, November, 21-26, 1988

[9] G. Sissoko, C. Museruka, A. Corréa, I. Gaye and A. L. Ndiaye,. Light spectral effect on recombination parameters of silicon solar cell. Renewable Energy. 3: 1487-1490. 1996.

[10] H. L. Diallo, A. Wereme, A. S. Maïga and G. Sissoko, New approach of both junction and back surface recombination velocities in a 3D modeling study of a polycrystalline silicon solar cell. Eur. Phys. J. Appl. Phys., 42: 203–11. 2008.

[11] G. Sissoko, E. Nanema, Y. L. B. Bocande, A. L. Ndiaye, M. Adj Minority carriers measurement in silicon solar cell under constant white bias light. World Renewable Energy Congress (WREC), Vol. 3, pp 1594-1597, 1996, Elsevier Science Ltd.

[12] I. Ly, O.H. Lemrabott, B. Dieng, I. Gaye, S. Gueye, M.S. Diouf, and G. Sissoko; Techniques for determining the recombination parameters and the validity domain of a bifacial polycrystalline silicon solar cell under constant multispectral illumination in static regime. Review of Renewable Energy; Vol. 15 N°2 (2012) 187 – 206.

[13] Nd. Thiam, A. Diao, M. Ndiaye, A. Dieng, A. Thiam, M. Sarr, A.S. Maiga and G. Sissoko. Electric Equivalent Models of Intrinsic Recombination Velocities of a Bifacial Silicon Solar Cell under Frequency Modulation and Magnetic Field Effect Research Journal of Applied Sciences, Engineering and Technology (Published: November 15, 2012). Vol. 4, (22): 4646-4655.

[14] G.Sissoko, C. Museruka, A. Correa, I. Gaye, A. L. Ndiaye. Light spectral effect on recombination parameters of silicon solar cell. World Renewable Energy Congress (1996), part III, pp.1487-1490

[15] I. ly, M. Ndiaye, M. Wade, N. Thiam, S. Gueye and G. Sissoko; Concept of Recombination Velocity Sfcc at the Junction of a Bifacial Silicon Solar Cell, in Steady State, Initiating the Short-Circuit Condition; Research Journal of Applied Sciences, Engineering and Technology 5(1): 203-208; ISSN: 2040-7459; e-ISSN: 2040-7467; 2013.